Hydrol. Earth Syst. Sci. Discuss., doi:10.5194/hess-2016-362, 2016
Manuscript under review for journal Hydrol. Earth Syst. Sci.
Published: 30 August 2016

Hydrology and Earth System Sciences
Discussions

Urban sewershed overflow analysis using super-resolution weather radar rainfall

J. Y. Hyun[1], T. D. Rockaway[1] and M. N. French[1]

[1]{University of Louisville, Louisville, Kentucky}

Correspondence to: J. Y. Hyun (j0hyun01@cardmail.louisville.edu)

Abstract

In urban areas, a prevalence of combined sewer systems (CSS) exist that carry both storm water runoff and sanitary sewer flows in a single pipe, these system are considered combined sewers. In the absence of rainfall-runoff most of these systems function adequately, however CSS capacity is typically inadequate to carry peak stormwater runoff volume. In order to minimize sewage flooding into streets and backups into homes and businesses, most CSS (as well as separate sanitary sewer system) are designed to overflow into surface waters such as streams and rivers, lakes and seas.

The primary factor causing overflows to occur is excessive precipitation with rainfall at high intensity or high volume. A framework for the application of radar-rainfall data to identify rainfall characteristics (spatial and temporal) associated with CSO events is presented in this work. An innovative component of the work is the identification of a relationship between weather radar reflectivity and ground-level rainfall. Additionally, the sewershed specific radar-rainfall region is extracted for use in defining CSO triggering rain event characteristics at sewershed spatial scale. Results show underestimation of rainfall is more problematic than overestimation. An optimal radar-rainfall relationship is developed to address reflectivity (Z) to rainfall (R) transformation and improves rainfall estimates in the higher reflectivity range (greater

Hydrol. Earth Syst. Sci. Discuss., doi:10.5194/hess-2016-362, 2016
Manuscript under review for journal Hydrol. Earth Syst. Sci.
Published: 30 August 2016

or equal to 46 dBZ). A large portion of quarter-hourly rainfall accumulations occurring at lower radar reflectivity, less than 46 dBZ, indicate optimal reflectivity-rainfall (Z-R) relation parameters range from [300, 1.4] to [250, 1.4] for convective storm types, and [250, 1.2] to {[80, 1.4], [120, 1.4]} for tropical rainfall types. Both rainfall and overflow events are identified using criteria proposed by United States Environmental Protection Agency (USEPA) to define the physical continuity of natural rainfall processes and the corresponding hydrologic response. The methodology framework is illustrated using an urban sewershed, denoted as CSO 130, located in Louisville, Kentucky (USA). The role of specific rainfall event characteristics: total volume, intensity, duration, continuity, and storm types are shown to govern the overflow in the approximately 13-ha (30-ac) sewershed. Through discriminant analysis, the coupled rainfall and overflow events are categorized by overflow severity. Results indicate that use of fine-resolution radar-rainfall in this urban hydrologic system can reveal insights for planning CSO control and prevention measures for specific rainfall event regimes.

1. Introduction

In many urban areas, combined sewer systems (CSS) carry both storm water runoff and sanitary sewer flows in a single pipe. In the absence of rainfall-runoff most CSS adequately convey waste water flow, however system capacity may be overwhelmed when it must also transport significant stormwater runoff. In order to prevent sewage from flooding streets and backups into homes and businesses, most CSS (as well as separated sanitary sewer systems) are designed to overflow into surface waters such as streams and rivers, lakes and seas. This overflow occurrence is considered a combined sewer overflow (CSO) event and has a detrimental impact on aquatic environments and degrades downstream water quality.

Hydrol. Earth Syst. Sci. Discuss., doi:10.5194/hess-2016-362, 2016
Manuscript under review for journal Hydrol. Earth Syst. Sci.
Published: 30 August 2016

In the United States (USA), regulations were established to eliminate CSO events in urban areas (EPA 1994). Although CSS are now considered an outdated approach to waste water collection, these legacy water collection systems form a considerable portion of the sanitary sewer network in the United States. It is estimated that 860 communities across the USA are served by combined sewer systems with over 10,000 CSO outfalls directed into natural surface waters. These communities include approximately 40 million people in more than 30 states (EPA 2004). The direct solution to eliminate overflow occurrence through modification or replacement of CSS with separate sewer and storm drains is cost prohibitive, disruptive to the community, and difficult or infeasible to accomplish in existing urban environments (Lyandres and Welch, 2012). When a CSO event occurs, the effect on receiving waters can be significant. The overflow transports microbial pathogens, oxygen depleting substances, suspended solids, toxics, nutrients, and debris including floatables and trash directly into the natural aquatic environment (EPA 2004). Furthermore, in most urban areas CSO occurrence is often a sudden phenomenon, due to both characteristics of the triggering rain storm and hydrologic conditions in the sewershed, resulting in a surge of runoff (Romnée et al. 2015).

Understanding the role of CSO triggering precipitation events is considered in previous studies on the relationship between rainfall and CSO occurrence. Recent work by Mailhot et al. (2015) developed a relation between annual duration of overflow occurrence and rainfall threshold category derived from rain gauge data. Mailhot et al. (2016) describe the value of rainfall data in terms of spatial co-location and temporal coincidence, and mention the limitations of rain gauge data in evaluation of CSO occurrence. The work of Mounce et al. (2014) includes radar-rainfall information and focuses on forecasting CSO occurrence and less on identification of catchment-scale rainfall characteristics. Both Montalto et al. (2007) and Lucan and Sample (2015) incorporate scenarios of runoff modeling

Hydrol. Earth Syst. Sci. Discuss., doi:10.5194/hess-2016-362, 2016
Manuscript under review for journal Hydrol. Earth Syst. Sci.
Published: 30 August 2016

using modified forms of traditional design rainfall derived from regional climatology to illustrate the performance impact of a variety of Green and LID (low impact development) strategies on CSO occurrence.

This work moves toward understanding rainfall through downscaling in urban areas as a means to identify specific rain event spatio-temporal characteristics. A occurrence may be improved by defining fine spatiotemporal resolutions. The challenge in CSO mitigation however, is that for most sewersheds, common operationally measured rainfall characteristics (rain event duration, total rain volume, intensity, continuity (inter-event time, IET), seasonality and storm type (e.g., stratiform, convective, frontal, orographic, tropical storm remnants), are determined based on spatially distant point source rain gauges and lack catchment specific detail. Data records with relevant spatial and temporal details describing precipitation variability is necessary to define the characteristics of storm events triggering CSO events.

Historically, rainfall monitoring by ground-level rain gauge networks is considered a reliable measurement system for many hydrologic applications because it physically captures pluvial water. In hydrologic engineering and research, rain gauge measurements frequently serve as a reference for evaluation of indirect or remote sensing rainfall estimation systems such as weather radars and satellites (Habib et al., 2012; Price et al., 2014; Chen et al., 2015; Fencl et al., 2015). Several recent studies have utilized existing rain gauge data from single points or networks. However, the detection of spatial rainfall variation by gauge networks is limited, in particular at finer temporal resolution. Qi et al. (2016) studied the quality control of a rain gauge network of hourly data to alleviate error sources. Girons Lopez et al. (2015) focused on spatial variation of the rainfall for a sizeable watershed (30000 km^2). Gianotti et al. (2013) mentions the limitation of rain gauges use in seasonal weather prediction. Based on

Hydrol. Earth Syst. Sci. Discuss., doi:10.5194/hess-2016-362, 2016
Manuscript under review for journal Hydrol. Earth Syst. Sci.
Published: 30 August 2016

these studies, indications are that both rain gauge location and data quality control are important. The focus of this study is application of radar and rain gauge data in the small-scale sewershed and consideration of spatial variation. Additionally, a fine temporal resolution is maintained to preserve coincidence of rainfall and peak overflow variation and reduce information loss. Thus, this study includes characteristics of localized rainfall events, which may vary significantly from spatial averages, through use of radar-rainfall products and therefore explicitly incorporates rainfall spatial variation.

Hydrometeorologic rainfall monitoring and measurement technology of the weather radar has advanced in recent decades (Karamouz and Nazif, 2013; Morita, 2011; Yang et al., 2013). While existing research has been directed to developing Z-R relationships for one-hour rainfall accumulations (Baeck and Smith, 1998), this study focused on linking radar reflectivity to rain gauge networks for short duration applications (less than one-hour). By synchronizing radar rainfall with rain gauge measurements the dependency (and associated uncertainty) of the Z-R conversion on storm type classification (convective, tropical, east cool stratiform and stratiform) is diminished. Unfortunately, the Z-R relationship is not typically calibrated for a particular hydrologic climate or rainfall type and no real-time automated optimization is implemented (Chumchean et al., 2003; Ice, 2014). Synchronizing radar reflectivity data with the rain gauge network, a more precise estimate of rainfall (depth, spatial and temporal variations) indicate improved rainfall estimates at scales of 0.5 km^2 and 0.5 hours. In this study, support vector classification (SVC) is used to partition storm events by underlying characteristics and includes an optimization process for Z-R parameter estimation; the radar-rainfall data are areal rainfall observations at the sub-hectare (radar polar coordinate pixel size) resolution at sub-hour temporal intervals.

Hydrol. Earth Syst. Sci. Discuss., doi:10.5194/hess-2016-362, 2016
Manuscript under review for journal Hydrol. Earth Syst. Sci.
Published: 30 August 2016

Identification of rainfall events, for example, using the EPA criteria for urban areas and a defined inter-event time (IET), provides a context for identifying rainfall spatial and temporal characteristics associated with CSO overflow events. Accordingly, preparation of accurate rainfall data, quality controlled weather radar data, identification of independent rainfall events and corresponding CSO event hydrographs are essential to developing a quantitative understanding of the phenomenon.

To this end, an objective for this study includes application of locally optimized radar-rainfall to an urban sewershed (watershed) using fine-scale spatiotemporal resolution data, and evaluation of rain event characteristics resulting in CSO events. This work generates a coincident data set of coupled radar-rainfall-CSO events. Categorization of the severe rainfall events inducing CSO occurrence can provide insights for hydrologic and hydraulic design guidelines to reduce sewer overflows from combined sewer systems in an urban area.

2. Local weather radar optimization

2.1. Radar rainfall source and preprocessing

The study region for this work is the city of Louisville, Kentucky (USA) during the period January 2010 to December 2014. Rainfall data from an operational rain gauge network, managed by the local utility agency Metropolitan Sewer District (MSD), are the ground reference values (Hyun et al., 2016). The region's Next-Generation Radar (NEXRAD) (denoted by call letters KLVX) is located at Fort Knox, Kentucky about 40-km southwest of the city of Louisville.

In case studies of rainfall spatiotemporal structure, a correlation near 0.6 at 5-km distance for quarter-hour temporal resolution using ground based rain gauges is shown (Ciach and Krajewski, 2006; Jung et al., 2014; Mandapaka and Qin, 2013). The average inter-gauge

Hydrol. Earth Syst. Sci. Discuss., doi:10.5194/hess-2016-362, 2016
Manuscript under review for journal Hydrol. Earth Syst. Sci.
Published: 30 August 2016

144 distance in this application is slightly greater and the gauge network can therefore benefit
145 from the complementary spatial detail provided by weather radar. Although the radar data are
146 not explicitly filtered for error adjustment, the large quantity of data compiled for use, from
147 gauge network and radar archives, is expected to minimize bias. Additionally, the proximity
148 of the study area relative to the radar site, at about 40 km range, is expected to diminish the
149 influence of common radar error influences such as range effects of signal attenuation,
150 anomalous propagation, beam blockage, and beam spreading (Ciach et al., 2003; Gorgucci
151 and Baldini, 2015; Hunter, 1996; Kalogiros et al., 2013; Krajewski and Vignal, 2001; Morin
152 et al., 2003; Seo et al., 2000; Vignal and Krajewski, 2001).

153 The fifteen rain gauges of the MSD network are mechanical tipping-bucket type with
154 resolution of 0.01 inch and temporal interval of five minutes. The data records for radar base-
155 scan reflectivity (Level II - NEXRAD dual polarization, 0.5 dBZ increment) were retrieved
156 from the National Climatic Data Center (NCDC) at National Oceanic and Atmospheric
157 Administration (NOAA). The data cover the entire five-year study period, 2010-2014, in the
158 format of coded reflectivity volume scans. The raw reflectivity was converted to a Cartesian
159 coordinate (ESRI ASCII grid files) system using NCDC's Weather and Climate Tool Kit
160 (WCT), version 3.7. The WCT provides visualization and export tools to manipulate radar
161 data. The Constant Altitude Plan Position Indicator (CAPPI) data, 1-km above the radar
162 elevation, forms the base-scan reflectivity array over the study area. The spatial pixels are
163 approximately 220-m square in a Cartesian coordinate grid over the study area, thus pixel area
164 is less than 5-hectare (15-acre).

165 The raw radar reflectivity data are instantaneous values and require conversion to
166 rainfall intensity and accumulation to define volumetric rainfall. In order to geo-synchronize
167 reflectivity pixel locations with reference network gauge locations, radar reflectivity pixels

Hydrol. Earth Syst. Sci. Discuss., doi:10.5194/hess-2016-362, 2016
Manuscript under review for journal Hydrol. Earth Syst. Sci.
Published: 30 August 2016

168 with spatial locations corresponding to MSD gauge locations were identified. In the same
169 vein, a temporal synchronization was performed to identify radar scan time stamps
170 corresponding to the local time zone (accounting for daylight savings time as appropriate).
171 For each rain gauge site, the collocated radar pixel and adjacent eight pixels were identified
172 for use in data evaluation. Among these nine radar pixels, the single collocated radar pixel
173 value was selected when reflectivity was within 50% of the average of surrounding pixel
174 values. Where the difference between the center pixel value and surrounding values was
175 more than 50%, the averaged reflectivity value was assigned. In the case where a majority of
176 the 9 radar reflectivity data showed a status or condition as "not available" the pixel status
177 was defined "not available".

178 The KLVX radar data management system applies a Z-R relationship according to
179 four storm types: convective, tropical convective, stratiform, and east cool stratiform.
180 Reflectivity transforms into rainfall intensity as an instantaneous value, whereas the gauge
181 values are demonstrate accumulated rainfall over five minutes (Ulbrich and Lee, 1999).
182 Therefore, instantaneous intensity is further transformed into accumulated rainfall following
183 application of the Z-R relationship. The first step considers all four reflectivity to rainfall
184 intensity (mm/hr) conversions. Additionally, temporal synchronization was required since
185 radar observations are not recorded at equal or uniform temporal intervals. Instead,
186 reflectivity scan intervals cover a 4- to 10-minute range due to the operational mode of the
187 weather radar. Generally, three or four instantaneous base scans cover the quarter-hourly
188 period, and each volumetric scan is weighted according to the inter-scan time interval within
189 the quarter-hour interval. The process is defined in Equation (1) (Appendix) based on a
190 weighted time of occupation for each scan within the quarter-hourly interval. For each
191 reflectivity volume scan, the time interval is defined as the duration from the observation until

Hydrol. Earth Syst. Sci. Discuss., doi:10.5194/hess-2016-362, 2016
Manuscript under review for journal Hydrol. Earth Syst. Sci.
Published: 30 August 2016

192 the next observation recorded (inter-scan interval) or the end of the fifteen-minute
193 accumulation window.

194 Figure 1 illustrates the volumetric radar rainfall products at monthly to quarter-hour
195 temporal resolutions. The quality of quarter-hourly radar rainfall estimation is relatively low
196 while hourly and longer accumulated rainfall products reveal better agreement with gauge
197 rainfall. However, this study focuses on the shorter duration, quarter-hourly interval, in order
198 to illustrate radar rainfall products for use in smaller urban catchment applications (Cunha et
199 al., 2015; Krajewski et al., 2010; Smith et al., 2007; Wright et al., 2014). In Figure 1, most
200 data are found at the depth range of 5 mm or less for quarter-hourly rainfall because rain
201 gauge data reliability and detection is sensitive during light rainfall (Ciach, 2002; Humphrey
202 et al., 1997). For these reasons, a quarter-hour rainfall accumulation threshold of 5 mm was
203 implemented for evaluating the Z-R relationship in the remaining portion of this study.

204 **2.2. Radar rainfall optimization by support vector classification**

205 Application of the optimal Z-R relationship, selected as the one yielding lowest Root-
206 Mean-Square-Error (RMSE), for each 15-min rainfall accumulation and each rainfall type
207 category, is summarized in Figure 2 (origin at 5mm rainfall threshold). The rain type
208 categories corresponding to tropical and east cool stratiform show a dispersed result.
209 Conversely, the convective and stratiform types tend toward agreement with gauge values as
210 indicated by the lower variance and narrower clustering along the one-to-one line. Further
211 optimization processes are considered for the stratiform type rainfall values since the result
212 shown is considered adequate for this work. In the case of east cool stratiform type, most
213 rainfall depths are less than 10 mm, and this depth is less significant from a hydrologic runoff
214 generation perspective. For this reason, the east cool stratiform rainfall type is not considered
215 in the remaining part of this study. This leaves convective and tropical type rain categories

Hydrol. Earth Syst. Sci. Discuss., doi:10.5194/hess-2016-362, 2016
Manuscript under review for journal Hydrol. Earth Syst. Sci.
Published: 30 August 2016

for consideration, and the focus is on development of an optimization process to improve agreement of radar-based and gauge-measured rainfall accumulation.

Figure 3 presents a comparison of the convective storm type radar depths and the gauge rainfall depths. The lighter shaded markers indicate use of the standard Z-R transformation with parameters (a:300, b:1.4) and the darker marker dots indicate the optimized Z-R result. A simplex optimization procedure was applied to optimize the Z-R parameters over value ranges of 10 to 500 and 0.5 to 3 for a and b respectively. Optimization decreased RMSE and Z-R parameters values of 300 and 1.4 were modified to 250 and 1.4 for a and b respectively. The optimized Z-R parameters eliminated the systematic underestimation but the dispersion is unchanged; the simplex optimization centered all values about the one-to-one line.

The tropical convective rainfall type contains a large number of high intensity values and has the widest spread of the comparison groups. An interesting and challenging issue is that bias cannot be eliminated by calibration of the Z-R parameters alone. As shown in Figure 4 (upper-left), underestimation of rainfall remains following optimization of Z-R parameters a and b. In Figure 2 (upper-right, red), the result is shown for the best fit Z-R, yet the tropical type rainfall appears to form two distinct groups. The first group is slightly above the one-to-one line with limited dispersion, whereas a second group is under the one-to-one line with wider variability. This indicates that a single Z-R relationship for tropical type may not suffice to encompass the observed characteristics of tropical type rainfall for this region.

In order to investigate a solution for this issue, a SVC optimization procedure was developed. The SVC optimization incorporates an unsupervised learning algorithm applied in the context of a two dimensional surface (x-axis: gauge rainfall and y-axis: radar rainfall). The concept is a data-based learning process; the SVC creates a linear hyperplane separating

Hydrol. Earth Syst. Sci. Discuss., doi:10.5194/hess-2016-362, 2016
Manuscript under review for journal Hydrol. Earth Syst. Sci.
Published: 30 August 2016

two binary groups according to a separation margin criteria. The hyperplane forms a linear separation at the maximum margin and is highly efficient in differentiating the non-linear rainfall characteristics. The determinant in the SVC is a kernel method transformation into a feature vector (Cristianini and Shawe-Taylor, 2003). In Figure 4 (upper-right), the maximum instantaneous reflectivity among the group of influential reflectivity values for quarter-hourly rainfall accumulation defines the kernel. The averaged radar rainfall error (difference from gauge value) is at the range of 44 dBZ to 47 dBZ and reflectivity of 46 dBZ is selected in order to balance the number of data values in each group. The kernel method is described in Equation (2) in the Appendix and defines the two groups through the linear hyperplane. The similarity function of the kernel method follows training data instead of a fixed set of parameters, and this feature involves the similarity function k, denoted as kernel in Equation (2). More simply, the kernel is a weighted sum of similarities between the trained example input and the new unknown input. The kernel is used as a binary classifier in terms of $\hat{y}$, the binary classifier for clustering the two tropical groups. In Figure 4 (lower-left) the linear hyperplane shows two data groups, one group fit with the tropical type Z-R relationship and the second group in the underestimated region. Following the SVC process, calibration of the Z-R parameters (RMSE minimum) was completed and the result is shown in Figure 4 (lower-right). This result demonstrates gains in information for the tropical type rainfall when two Z-R parameter sets (a, b) are used. The original fan-shaped dispersion is greatly reduced, as well as the original underestimation issue. The SVC-based solution process provides a multi-category classification and overcomes limitations of binary classification (Xie et al., 2013).

Use of an uncalibrated Z-R relationship for conversion of reflectivity to rainfall intensity for short-duration accumulations may result in differences from ground-level rain gauge observations. An example of these differences is presented in Figure 5 (upper-left) where results show a fan-shaped spreading with correlation of 0.68 between gauge and radar

Hydrol. Earth Syst. Sci. Discuss., doi:10.5194/hess-2016-362, 2016
Manuscript under review for journal Hydrol. Earth Syst. Sci.
Published: 30 August 2016

265 rainfall. Coincidentally, underestimation of rainfall may be more problematic than
266 overestimation in applications of hydrological management and design, and this result is
267 relevant for the tropical type rainfall category. In Figure 5 (upper-left), the comparison shows
268 the best fit standard Z-R relationship (minimum RMSE), and the tropical Z-R relationship
269 corresponding to the solid red line in Figure 5 (upper-right). This indicates the tropical Z-R
270 may not capture a complete description of rainfall variability at higher intensity rainfall rates.
271 This study introduced an alternate Z-R relationship formed using an SVC optimization
272 process. Use of the alternate Z-R relationship produced the results in Figure 5 (lower-left)
273 and Figure 5 (lower-right). A comparison of the alternate Z-R (red dotted line) and NWS
274 tropical Z-R (red solid line) relationships are included. This alternate Z-R relationship,
275 designated as "tropical-2", is more influential in the higher reflectivity range (greater or equal
276 to 46 dBZ). The Z-R relations shown in Figure 5 (lower-right) illustrate the placement of the
277 existing NWS tropical (tropical-1) Z-R relationship between the convective (black solid line)
278 and tropical-2 (red dotted line). Graphically, the tropical-1 relationship fills the gap between
279 the other two convective Z-R relationships. A notable point is that a large portion of the
280 quarter-hourly rainfall accumulations occurring at lower radar reflectivity, less than 46 dBZ,
281 are well represented by the tropical-1 Z-R relationship. The focus of this study on a relatively
282 shorter, quarter-hourly, rainfall accumulation interval, and the focus on more intense rainfall
283 values are factors influencing the need to partition this extreme- type rainfall (NWS tropical)
284 into two sub-groups.

285 In general, the two tropical sub-groups are similar in the low reflectivity range and
286 deviate more from one another for reflectivity above 45 dBZ to 50 dBZ. Based on the use of
287 categorized Z-R relationships in the region of more extreme rainfall intensity, quarter-hourly
288 rainfall estimation is improved with a correlation of 0.72 in Figure 5 (lower-left). For

Hydrol. Earth Syst. Sci. Discuss., doi:10.5194/hess-2016-362, 2016
Manuscript under review for journal Hydrol. Earth Syst. Sci.
Published: 30 August 2016

applications in urban hydrologic designs and simulation of historical events, the shorter temporal resolution of rainfall is useful.

3. CSO130 overflow analysis

3.1. Urban sewershed setting and CSO location

The sewershed CSO130 is part of the urban CSS and located in an older neighbourhood, called Buchertown, in Louisville, Kentucky. The specific location of CSO130 is along Webster Street and its overflow control structure type is a diversion dam. The sewershed is approximately 13-ha (30-ac) and land-use is a mixture of commercial and dense residential. The land-use is about 75% impervious with the portions distributed as residential (24%), commercial (25%), industrial (32%), vacant land (6%), and roads and other uses (13%). The CSO130 outfall discharges into the nearby stream, Beargrass Creek, which is a tributary of the Ohio River.

MSD operates a rain gauge network across the city region and one rain gauge is located near the study area. However, data from this gauge serves only as a reference to evaluate radar rainfall quality rather than as rainfall for the sewershed. The benefit and challenge of using weather radar data for operational applications is illustrated and the spatial variation of rainfall derived from weather radar products described. The radar records are extracted and optimized, with spatiotemporal resolution of quarter-hour and less than five-hectare (15-acre), in order to be applicable for the urban hydrologic scale.

3.2. Coupled radar rainfall and overflow event record

Only rain events resulting in a CSO event are considered and a quality control threshold is applied to select rain-overflow events exceeding a ratio of 0.60 for overflow

Hydrol. Earth Syst. Sci. Discuss., doi:10.5194/hess-2016-362, 2016
Manuscript under review for journal Hydrol. Earth Syst. Sci.
Published: 30 August 2016

depth to rainfall depth. Discriminant analysis is used to categorize the coupled rainfall-overflow events according to overflow severity; a threshold of the overflow depth of 1.5-mm partitions the event categories. Results indicate that overflow depth has a strong linear relationship with rainfall depth and other environmental factors are influential.

Identification of rainfall events, using the EPA criteria for urban areas and a defined inter-event time (IET), provides the context for identifying overflow events in the CSO flow record. Accordingly, preparation of accurate rainfall data, quality controlled weather radar data, and a record of independent rainfall events, are essential. In radar rainfall estimation, super resolution data are suitable to define rainfall variation over urban areas.

Figure 6 shows radar rainfall comparisons with gauge rainfall data sources near the study area. An MSD rain gauge, gauge number TR05, is located about 600-m away from the study area, and this data record is used as a reference to evaluate spatial variation of rainfall. The improved radar data shown in Figure 6 (upper-right) has improved the correlation to 0.79 compared with a 0.70 correlation in the original estimate (Figure 6 upper-left). Two other rain gauges, TR12 and TR03 show correlation of 0.55 and 0.05 with the TR05 data respectively. Within a distance of 15-km, rainfall is spatially uncorrelated (ρ=0.05), and correlation decreased to 0.55 within 5km distance at TR12. This reveals the high spatial variation of the rainfall at quarter-hourly temporal resolution and the benefit of radar-rainfall over the limitation of reliance solely on ground-based rainfall measurement.

The CSO mechanism in the sewershed is not only related to the rainfall characteristics; depth, duration and intensity, but also the continuity of the rainfall event. Figure 7 illustrates the extreme overflow cases at CSO130 in time-flow manner and the hydrologic response is related to rainfall variations within the rain event. The nine overflow events shown indicate that most were triggered immediately following the heaviest rainfall interval. Naturally, the

Hydrol. Earth Syst. Sci. Discuss., doi:10.5194/hess-2016-362, 2016
Manuscript under review for journal Hydrol. Earth Syst. Sci.
Published: 30 August 2016

rainfall volume is the primary influence on overflow amount, but it is not the only factor. The more sizeable rainfall peaks affect the overflow amount and time distribution. For example, the sixth greatest overflow in Figure 7, with overflow amount of 10.68-mm, has precipitation duration less than an hour but the overflow was significant because of high intensity rainfall. On the contrary, the overflow event which ranked in fourth has no clear intense rainfall observed; instead rainfall is steady and uninterrupted. These results indicate rainfall event continuity as another factor triggering overflow event occurrence.

One definition of a rainfall event is provided by the EPA for rainfall event in the context for urban regulatory settings (Driscoll et al. 1989). The EPA document defines a rainfall event as "A minimum storm volume of 0.1-inch (2.54-mm) was specified for the analysis that were performed, so that the analysis would produce statistics of 'runoff producing' events within 6 hours." In short, a single rainfall event is completely independent if no sizeable rainfall, greater than 2.54-mm (0.1-inch), occurs within six hours. The rainfall event defined by EPA regulation and corresponding time for the overflow event were determined from the time rainfall began until six hours from the end of the rainfall event. By EPA definition, a rainfall event is followed by at least a six-hour dry period and so the implied time available for overflow to occur is limited to six hours following the rain event. Based on this, there are 95 rain events with coupled CSO occurrence in the sewershed for CSO130 over the three-year study period, January 2011 to December 2013.

3.3. CSO130 overflow analysis

The CSS CSO130 control structure is a 0.61-m (24-inch) circular brick sewer pipe flowing with an average of 12 overflow incidents (events) per year (averaged 2.33 hours of duration and 90,000 gallons of combined sewer per incident) (MSD, 2014).

Hydrol. Earth Syst. Sci. Discuss., doi:10.5194/hess-2016-362, 2016
Manuscript under review for journal Hydrol. Earth Syst. Sci.
Published: 30 August 2016

3.3.1. Quality control of coupled rainfall/overflow event

The number of CSO events identified directly from data records of rainfall and overflow analysis indicates the number of incidents is 95, and this is a greater number than the 35 to 40 otherwise expected according to the average number of reported incidents over the same three-year study period (MSD 2104). Potentially, the method of identification and event partitioning (IET) may influence the number, but proper quality confirmation is required for data reliability. To this end, a means of screening outliers and poor quality data records is utilized. Application of a common rainfall-runoff index threshold screening, based on watershed characteristics, is not possible since the total runoff for each CSO event partitions flow into two directions, one part is the overflow and the remaining portion continues to the water treatment plant. During an overflow event it is not possible to separate the portion attributed only to stormwater runoff. To address this issue, CSO event data are partitioned into acceptable and non-acceptable clusters. Figure 8 (left) shows the normalized runoff-rainfall index ratios of overflow depth to radar-rainfall depth and overflow depth to gauge rain depth for each event. The plot spreads in a two-dimensional field; with x-axis: ratio for rain gauge MSD TR05 (600m from CSO130), and y-axis: ratio for radar rainfall. A ratio greater than 1 indicates runoff greater than rainfall, and this unlikely occurrence may indicate data error or other issues; for this reason, these data are excluded from the study. The use of two rainfall sources lessens the uncertainty concerning rainfall occurrence and incorporates both these practical hydrologic observations into this study. Figure 8 shows a notable absence of overflow occurrence between ratio values of 0.60 and 0.80. Therefore, a threshold ratio of 0.60 was defined as the acceptable coupled rainfall and overflow event criteria; this is the boundary where data are densely populated and shown as the inner region defined by a bold solid line forming a quarter-circle in Figure 8 (left). The right portion of Figure 8 shows all CSO events and the bold solid line indicates a value of 0.6 for the radar

Hydrol. Earth Syst. Sci. Discuss., doi:10.5194/hess-2016-362, 2016
Manuscript under review for journal Hydrol. Earth Syst. Sci.
Published: 30 August 2016

overflow ratio. The result identifies two groups of CSO events: acceptable (blue) and non-acceptable (red). This process indicates 52 coupled rain-overflow events and this corresponds well with the expected number as suggested by the MSD report for the three-year study period (MSD, 2014).

3.3.2. Analysis of coupled rainfall and overflow events

3.3.2.1. Overflow relation to rainfall depth, intensity and duration

The coupled rain and overflow record for CSO130 shows the sewershed runoff response is prompt with a hydrograph form similar to a smoothed and time-lagged reflection of the hyetograph. That being so, understanding the rain event characteristics provides insights into the timing, intensity and amount of overflow. Fundamentally, the quantitative relation between rainfall and overflow has a visible linearity as in Figure 9 (left). Rain volume is an important factor and shows a linear relationship with overflow. As shown in Figure 9, when rainfall is less than about 8-mm a low overflow volume occurs and overflow amount increases linearly above this rainfall depth. For overflow values above a 0.40 ratio of rainfall volume the sewer overflow volume is more significant and likely to impact environmental quality in the Beargrass Creek. It is expected that total rainfall depth is a significant factor triggering an overflow, but this simplified conclusion cannot completely explain the behaviour and a search to understand the contributing factors causing overflow events is warranted.

The rain event duration and peak intensity (15-minute temporal resolution) are important in determining overflow volume in Figure 9 (right). In the duration versus rainfall depth field (Figure 9 right), the events clearly divide into two groups when clustered by peak rainfall intensity. The two groups have somewhat different tendencies in the two-dimensional

Hydrol. Earth Syst. Sci. Discuss., doi:10.5194/hess-2016-362, 2016
Manuscript under review for journal Hydrol. Earth Syst. Sci.
Published: 30 August 2016

space with the strong peak intensity group showing a relatively short duration but larger volume of rainfall. On the other hand, rainfall volume tends to be relatively stable and less relevant as an overflow trigger no matter the event duration. In the small-scale urban watershed setting, existence of high-intensity peak rainfall may produce significant volumetric rainfall, thus, rainfall intensity significantly impacts drainage system performance in urban areas (Arnbjerg-Nielsen et al., 2013; Mamo, 2015). Considering this result in a practical application, rainfall depth, intensity and duration are all factors indirectly incorporated into historic intensity-duration-frequency (IDF) curve used to define volumetric rainfall for urban hydrologic design. However, variations between rainfall observations and IDF design values illustrates the uncertainty for applications requiring fine spatiotemporal resolution such as urban sewersheds where runoff response occurs well under the sub-hour temporal scale.

3.3.2.2 Overflow relation to rainfall depth, storm type and continuity of rain

There is a thread of inter-connection between instantaneous heavy rainfall, storm type and resulting overflow in this small watershed. A concurrence of rainfall characteristics and watershed condition, for instance, existing antecedent moisture, wet or dry surfaces and soils, which effect rainfall retention and percolation, may influence overflow occurrence. Therefore, rainfall continuity in terms of single events is considered as an additional factor. The extreme overflow events in Figure 7 reveal the importance of the rainfall continuity since there are four high ranked overflows (rank number: 3, 4, 8, and 9) associated with rainfall events with relatively insignificant peak intensity (below 5-mm/15minute), but continuous and uninterrupted rainfall. In other words, the length of the duration of rainfall within a single event is an influencing factor related to the CSS capacity and resulting CSO for this sewershed.

Hydrol. Earth Syst. Sci. Discuss., doi:10.5194/hess-2016-362, 2016
Manuscript under review for journal Hydrol. Earth Syst. Sci.
Published: 30 August 2016

The ratio of the time rain falls during a rain "event" to total event duration represents the continuity of the rainfall or rainfall occupancy ratio. Figure 10 (left) illustrates the relationship between rainfall depth and rainfall occupancy by rain type and season; warm season (April to September) and cold season (October to March). The radar rainfall product indicates rainfall type for each 15-minute rainfall accumulation. The characteristics of a single storm, in motion over CSO130 sewershed, are dynamic and a series of storm cells may move over the area. The convective storm type may have a single or multiple cells within the developed storm structure associated with severe rainfall (Caine et al, 2013; Cetrone and Houze, 2006; Feng et al., 2014; Peter et al., 2015; Zawilski and Brzezińska, 2014).

Identification of rainfall type is based on the ratio of number of convective type radar pixels to total rain pixels in the storm. Applying a threshold ratio of 0.45 results in the two event groups; a convective prevalence group and a stratiform prevalence group. The stratiform group has no discernible spatial pattern features other than the continuity of rainfall coverage, while the convective group has a tendency toward increasing intensity beginning around a ratio of 0.60. The highest three rain depth events are in the convective group. The reappearance of the rainfall overflow plot (Figure 10, right), with seasonal rainfall group details added, demonstrates the characteristics of the overflow inducing rainfall events. Prior to presentation of this figure, the nine ranked overflow inducing rainfall events show a 0.81 ratio of rainfall occupancy and no event with lower than a 0.60 ratio. This indicates the rainfall event group most likely to generate a CSO are the convective rain group in summer season. The mitigation of combined sewer overflow events can use this information in hydrologic design to improve future approaches to stormwater runoff reduction. The overflow of CSO130 is a response to the interaction of natural rainfall variability, the urban landscape, land-use and hydrologic environment. In addition to rainfall variability, other qualitative factors influence the likelihood of overflow occurrence. Therefore, understanding the

Hydrol. Earth Syst. Sci. Discuss., doi:10.5194/hess-2016-362, 2016
Manuscript under review for journal Hydrol. Earth Syst. Sci.
Published: 30 August 2016

457 temporal and spatial structure of overflow inducing rain events is useful to estimate overflows
458 in CSOs.

459 **3.3.2.3 Discriminant analysis in overflow inducing rainfall events**

460 This study shows that an overflow event in a sewershed is induced through the
461 integration of factors from two fields; natural rainfall variability and the constructed
462 sewershed conditions. The fundamental assumption is that rainfall induces the overflow event
463 in a small-scale sewershed because the runoff response is rapid and the hydrograph structure
464 resembles the hyetograph. Thus, preventing overflow events inevitably requires
465 understanding of rainfall characteristics. The volumetric rainfall depth was shown to relate
466 linearly with overflow and other factors, such as rainfall intensity, duration, and continuity of
467 rainfall (as a ratio of rainfall occupancy) as influential factors. Discriminant analysis is
468 introduced to classify these precipitation factors. The discriminant analysis uses the
469 combination of features from the continuous independent variable (rainfall characteristics) to
470 define a separation of the discrete dependent variable (Martinez and Kak, 2001; Tahmasebi et
471 al., 2010) and is applied broadly in water resource (Sangam et al., 2008, Boyacioglu, 2010).
472 In order to apply discriminant analysis, the dependent variable (overflow) must be categorical
473 unlike the continuous independent variables. In Figure 11, a threshold overflow depth set at
474 1.5-mm, for the CSO130 sewershed, and categorizes the coupled rainfall-overflow events into
475 two groups; a significant overflow group (23 events referred to as group-1) and non-
476 significant overflow group (29 events referred to as group- 0).

477 In Table 1, the mean values of the rainfall related variables influencing the overflow
478 events are presented in discriminant groups. As expected, this highlights differences between
479 groups and provides a quantitative distinction of the decisive overflow factors. The mean
480 rainfall depth is 8.85-mm in the non-significant group (group-0) and 23.70-mm in the

Hydrol. Earth Syst. Sci. Discuss., doi:10.5194/hess-2016-362, 2016
Manuscript under review for journal Hydrol. Earth Syst. Sci.
Published: 30 August 2016

481 significant group (group-1). Overall, volumetric rainfall governs the overflow in this small
482 scale sewershed. The peak rain intensity has a similar tendency showing 3.76-mm per 15-
483 minute and 6.20-mm per 15-minute for group-0 and group-1, respectively. Commonly, the
484 rainfall depth and the rainfall intensity (peak) have positive correlation with overflow amount.
485 However, the duration of rainfall indicates a contrast to this expected result. In Figure 5
486 (right), the majority high rainfall depth events have shorter durations. These shorter rainfall
487 duration events are expected to fall into group-1 considering the relationship between rainfall
488 depth, intensity and overflow occurrence. In this case, the continuous, uninterrupted and
489 longer duration rainfall induces the overflow. This is due to the inverse correlation between
490 rainfall duration and rainfall continuity, where a correlation of -0.64 is indicated between
491 these independent variables. A longer rainfall duration is more likely to also contain a non-
492 rain period resulting in proportionally lower continuity.

493 Another matter that merits mention is the definition of rainfall event duration. The
494 study incorporates the USEPA (EPA, 2004) definition for continuous rainfall and independent
495 event identification. The emphasis is on whether event independence, using the temporal
496 separation of a six-hour dry period for a small-scale sewershed, is appropriate since both the
497 sequence of rain depth and continuity of rainfall within the rain event are influencing factors.
498 The differences are investigated here using discriminant grouping by rain type and rainfall
499 continuity, nevertheless overflow occurrence is associated more with rain events in group-1.
500 The definition of a rainfall event may be improved with incorporation of factors such as
501 watersheds size, land-use characteristics, and hydrologic goals.

502 Table 2 shows 78.8% (41 of 52) rainfall events are correctly classified using the linear
503 combinations identified by discriminant analysis. Under the predefined threshold overflow
504 depth of 1.5-mm, the 29 and 23 coupled events fall into non-significant and significant groups

Hydrol. Earth Syst. Sci. Discuss., doi:10.5194/hess-2016-362, 2016
Manuscript under review for journal Hydrol. Earth Syst. Sci.
Published: 30 August 2016

505 respectively. This threshold considered a balance for the number of events in each group. The
506 objective discriminant group clustering indicates 12 events in the significant group and 40
507 events in the non-significant group. The linear combination of rainfall factors, $\vec{w} \cdot \vec{\mu}$, include
508 the mean and variance for the clustered factors. The cluster grouping decision includes the
509 ratio of variances within and between the groups as defined by equation (3) (appendix).
510 Based on this formulation, each group was established by the lowest variance of rainfall
511 factors. The corresponding overflow depth is found to be about 4.6-mm for a rain event with
512 24-mm depth (single rain event category).

513 This type of information, specifically identifying overflow volume associated with
514 rainfall event characteristics, may serve as an indicator of overflow potential in a CSO
515 sewershed. Information defining a gradation of overflow potential may be useful for
516 operational optimization such as, real-time likelihood of an overflow occurrence, design of
517 overflow dam height or pipe size, or design of retro-fit infrastructure to mitigate significant
518 overflow events. In this study, CSO occurrence in a small-scale sewershed is investigated
519 with a focus primarily on rainfall characteristics.

520 **4. Conclusions and Future works**

521 Improving and preserving water quality and the aquatic environment in urban areas is a
522 focus of the EPA and a component of regulatory guidelines limits the allowable occurrence of
523 CSO (combined sewer overflow) events (EPA 1994, EPA 2004). The approaches for
524 mitigating overflow events require information to define existing CSO conditions and event
525 occurrence in terms of flow volume, seasonal variation, and pollutant type and concentration.

526 Use of an uncalibrated Z-R relationship for conversion of reflectivity to rainfall intensity
527 for short-duration accumulations may result in differences from ground-level rain gauge
528 observations. Coincidentally, underestimation of rainfall may be more problematic than

overestimation in applications of hydrological management and design, and this result is relevant for the tropical type rainfall category. This indicates the tropical Z-R may not capture a complete description of rainfall variability at higher intensity rainfall rates. This study introduced an alternate Z-R relationship formed using an SVC optimization process. This alternate Z-R relationship, designated as "tropical-2", is more influential in the higher reflectivity range (greater or equal to 46 dBZ). A notable point is that a large portion of the quarter-hourly rainfall accumulations occurring at lower radar reflectivity, less than 46 dBZ, are well represented by the tropical-1 Z-R relationship. For applications in urban hydrologic designs and simulation of historical events, the shorter temporal resolution of rainfall is useful.

The volumetric approach of CSS overflow event study in a small-scale sewershed is presented using the radar-rainfall characteristics. The study incorporates details of radar-rainfall data evaluation, rain event definition, and reveals the dependency of CSS overflow events on rainfall depth, duration, intensity, type and continuity. The radar derived rainfall is necessary to determine rain depth over the region of interest where the coverage of rain gauges is limited.

Fundamentally, a linear relation exists between rainfall and overflow depths governing the occurrence of CSO events in this small-scale sewershed. The identification of corresponding rainfall and overflow events requires evaluation of coupled rain-overflow events and the study determined an overflow depth to rainfall depth ratio of 0.60 indicative of valid events. The discriminant analysis clustered overflow events into overflow severity classes. The objective classification categorized most events correctly and the discriminant analysis provided an indication of the volumetric relationship between the rainfall and overflow in this sewershed system.

Hydrol. Earth Syst. Sci. Discuss., doi:10.5194/hess-2016-362, 2016
Manuscript under review for journal Hydrol. Earth Syst. Sci.
Published: 30 August 2016

The more significant sewer overflow events occur rapidly, typically within a few hours following rainfall and from rainfall event durations less than a half day. This means daily or longer rainfall records may not be suitable for overflow analysis for small-scale sewersheds. This is in part due to the lack of independence in the identification of overflow inducing rain events where rain intensity, rain continuity and variability definition within a single rain event are necessary. An in-depth investigation of rainfall and overflow relationships across a range of hydrologic settings and sewershed characteristics may reveal an index for the practical design of a sewer overflow prevention structures. This type of study is essential for optimal development of objective and quantitative methods to mitigate CSS overflows in urban environmental systems.

Appendix: Mathematical background

Equation (1)

$$\mathbf{R_Q(t,x)} = \sum_{\mathbf{i=1}}^{\mathbf{n}} \left(\frac{\mathbf{R_i}}{\mathbf{4}}\right)\left(\frac{\mathbf{t_{i+1}} - \mathbf{t_i}}{\mathbf{2}}\right)$$

where,

R_Q (t,x) is weighted accumulation of quarter hourly rainfall capsule at the fixed location where reference data are corresponded in arbitrary time, t

n is influential number of reflectivity values for R_Q (t,x) which fall into the quarter hourly capsule and front and the rear reflectivity value when it is influential to the capsule.

R_i is converted rainfall rate in millimeter per hour among four different NWS Z-R relationships

t_i is time of observation of instantaneous radar base scan

Equation (2)

Hydrol. Earth Syst. Sci. Discuss., doi:10.5194/hess-2016-362, 2016
Manuscript under review for journal Hydrol. Earth Syst. Sci.
Published: 30 August 2016

575 $$\hat{y} = \mathbf{sgn}\sum_{i=1}^{n} \mathbf{w_i y_i k(R_i, Ŕ)}$$

576 where,

577 $\mathbf{R_i}$ and $\mathbf{y_i}$ are instance-based learners for the i-th training example

578 $\mathbf{w_i}$ is a corresponding weight

579 Ŕ is an unlabeled input

580 k is a function of the weighted sum of similarities which is called kernel

581 $\hat{y}$ is a prediction label of kernelized binary classifier

582 Equation (3)

583 $$\boldsymbol{T} = \frac{(\vec{\mathbf{w}} \cdot \vec{\mu}_{\boldsymbol{Significant}} - \vec{\mathbf{w}} \cdot \vec{\mu}_{\boldsymbol{Non-Significant}})^{\mathbf{2}}}{\vec{\mathbf{w}}^{\boldsymbol{T}}\boldsymbol{COV}(\boldsymbol{R_{i,j}})_{\boldsymbol{Significant}}\vec{\mathbf{w}} + \vec{\mathbf{w}}^{\boldsymbol{T}}\boldsymbol{COV}(\boldsymbol{R_{i,j}})_{\boldsymbol{Non-Significant}}\vec{\mathbf{w}}}$$

584 where,

585 **T** is a decision factor for the clustering of Significant and Non-Significant groups of the overflow

586 event

587 $\vec{\mu_t}$ is mean value for the clustered group.

588 $\boldsymbol{R_{i,j}}$ is rainfall variables among rainfall depth, duration, intensity, type, continuity.

589

590 **Acknowledgements**

591 This sewershed study was partially supported by the MSD 'Green Infrastructure' project as a
592 co-operative study with the Center for Infrastructure Research at the University of Louisville.
593 We appreciate the reviewers for comments and suggestions that lead to an improved
594 manuscript.

595

596 **References**

597 Arnbjerg-Nielsen, K., Willems, P., Olsson, J., Beecham, S., Pathirana, A., Bűlow, G., I.,
598 Madsen, H.; Nguyen, V-T.-V, Impacts of climate change on rainfall extremes and urban
599 drainage systems: a review, Water Science and Technology, Vol. 68, Issue 1, p16-28, DOI:
600 10.2166/wst.2013.251, 2013

601 Baeck, M. L., Smith, J. A.: Rainfall Estimation by the WSR-88D for Heavy Rainfall Events,
602 Weather and Forecasting, AMS, Vol. 13, 1998

603 Boyacioglu, H.: Detection of seasonal variations in surface water quality using discriminant
604 analysis, Environmental Monitoring and Assessment, Vol. 162, p15-20, 2010

605 Caine, S., Lane, T. P., May, P. T., Jakob, C., Siems, S. T., Manton, M. J., and Pinto, J.:
606 Statistical assessment of tropical convection-permitting model simulations using a cell-
607 tracking algorithm, Monthly Weather Review, Vol. 141, Issue 2, p557-581,
608 DOI:10.1175/MWR-D-11-00274.1, 2013

609 Cetrone, J. and Houze, R. A.: Characteristics of tropical convection over the ocean near
610 Kwajalein, Monthly Weather Review, Vol. 134, Issue 3, p834-853, 2006

611 Chen, Y., Liu, H., An, J., Görsdorf, U. and Berger, F. H.: A field experiment on the small-
612 scale variability of rainfall based on a network of micro rain radars and rain gauges, Journal of
613 Applied Meteorology & Climatology, Vol. 54, Issue 1, p243-255, DOI: 10.1175/JAMC-D-13-
614 0210.1, 2015

615 Chumchean, S., Sharma, A., and Seed, A.: Radar rainfall error variance and its impact on
616 radar rainfall calibration, Physics and Chemistry of the Earth, Elsevier, Vol 28, p 27-39,
617 DOI:10.1016/S1474-7065(03)00005-6, 2003

618 Ciach, G. J.: Local Random Errors in Tipping-Bucket Rain Gauge Measurements, Journal of
619 Atmospheric and Oceanic technology, AMS, Vol 20, 2002

620 Ciach, G. J., Habib, E., and Krajewski, W. F.: Zero-covariance hypothesis in the error
621 variance separation method of radar rainfall verification, Advances in Water Resources, DOI:
622 10.1016/S0309-1708(02)00163-X, 2003

623 Ciach, G. J. and Krajewski, W. F.: Analysis and modeling of spatial correlation structure in
624 small-scale rainfall in Central Oklahoma, Advances in Water Resources-Elsevier,
625 doi:10.1016/j.advwatres.2005.11.003, 2006

626 Cristianini, N. and Shawe-Taylor, J.: An Introduction to Support Vector Machines and other
627 kernel-based learning methods, Cambridge University Press, Cambridge, UK, 2003

628 CSO characteristics report-Combined Sewer Overflow Fact Sheet (CSO130), Metropolitan
629 Sewer District (MSD), Louisville, Kentucky, 2014

630 Driscoll, E. D., Palhegyi, G. E., Strecker, E. W. and Shelley, P. E. (1989) "Analysis of storm
631 event characteristics for selected rainfall gages throughout the United States" National Service
632 Center for Environmental Publications (NSCEP), 1989, Environmental Protection Agency
633 (EPA), Washington DC

634 EPA: Environmental Protection Agency, Part VII, Combined Sewer Overflow (CSO) Control
635 Policy; Notice. Federal Register Vol. 59, No. 75, 1994

636 EPA: Environmental Protection Agency report to congress on impacts and control of
637 combined sewer overflows and sanitary sewer overflows, factsheet files/ 2015-
638 10/documents/csosso_rtc_ factsheet. Pdf, 2004

639 EPA, Report to Congress: Impacts and control of CSOs and SSOs, Environmental Protection
640 Agency, EPA 833-R-04-001, 2004

641 Fencl, M., Rieckermann, J., Sýkora, P., Stránský, D. and Bareš, V.: Commercial microwave
642 links instead of rain gauges: fiction or reality?, Water Science and Technology, Vol. 71, DOI:
643 10.2166/wst.2014.466, 2015

644 Feng, Z., McFarlane, S. A., Schumacher, C., Ellis, S., Comstock, J., and Bharadwaj, N.:
645 Constructing a merged cloud-precipitation radar dataset for tropical convective clouds during
646 the DYNAMO/AMIE experiment at Addu Atoll, Journal of Atmospheric & Oceanic
647 Technology, Vol. 31, Issue 5, p1021-1042, DOI: 10.1175/JTECH-D-13-00132.1, 2014

648 Gianotti, D., Anderson, B. and Salvucci, G. D.: What do rain gauges tell us about the limits of
649 precipitation predictability?, Journal of Climate, Vol. 26, Issue 15, p5682-5688, DOI:
650 10.1175/JCLI-D-12-00718.1., 2013

651 Girons Lopez, M., Wennerstrom, H., Norden, L. A. and Seibert, J.: Location and density of
652 rain gauges for the estimation of spatial varying precipitation, Physical Geography, Vol. 97,
653 Issue 1, p167-179, DOI: 10.1111/geoa.12094., 2015

654 Gorgucci, E. and Baldini, L.: Influence of Beam Broadening on the Accuracy of Radar
655 Polarimetric Rainfall Estimation, Journal of hydrometeorology, Vol 16, DOI: 10.1175/JHM-
656 D-14-0084.1, 2015

657 Habib, E., Haile, A. T., Tian, Y. and Joyce, R. J.: Evaluation of the high-resolution CMORPH
658 satellite rainfall product using dense rain gauge observations and radar-based estimates,
659 Journal of Hydrometeorology, Vol. 13, Issue 6, p1784-1798, DOI: 10.1175/JHM-D-12-017.1,
660 2012

661 Humphrey, M. D., Istok, J. D., Lee, J. Y., Hevesi, J. A., and Flint A. L.: A New Method for
662 Automated Dynamic Calibration of Tipping-Bucket Rain Gauges, Journal of atmospheric and
663 Oceanic technology, AMS, Vol 14, 1997

664 Hunter, S. M.: WSR-88D Radar Rainfall Estimation: Capabilities, Limitations and Potential
665 Improvements, Natl. Wea. Dig 20.4, p26-38, 1996

666 Hyun, J., Rockaway, T. D. and French, M. N.: Ground Rainfall Spatio-temporal Variation
667 Over Jefferson County, Kentucky: Case Study, Journal of Hydrologic Engineering, ASCE,
668 online publication, http://dx.doi.org/10.1061/(ASCE)HE.1943-5584.0001438, 2016

669 Ice, R. L., Heck, A. K., Cunningham, J. G., and Zittel, W. D.: Challenges of Polarimetric
670 Weather Radar Calibration. The eighth european converence on radar in meteorology and
671 hydrology, 2014

672 Jung, Y., Kim, H., Baik, J. and Chio, M.: Rain-gauge network evaluation using
673 spatiotemporal correlation structure for semi-mountainous regions, Atmospheric & Oceanic
674 Sciences, Vol. 25, Issue 2, p267-278, DOI: 10.3319/TAO.2013.10.31.01(Hy), 2014

675 Kalogiros, J., Anagnostou, M. N., Anagonostou, E. N., Montopoli, M., Picciotti, E., and
676 Marzano, F. S.: Correction of Polarimetric Radar Reflectivity measurements and Rainfall
677 Estimates for Apparent Vertical Profile in Stratiform Rain, Journal of applied meteorology
678 and climatology, Vol 52, DOI: http://dx.doi.org/10.1175/JAMC-D-12-0140.1, 2013

679 Karamouz, M. and Nazif, S.: Reliability-based flood management in urban watersheds
680 considering climate change impacts, Journal of Water Resources Planning & Management,
681 Vol. 139, Issue 5, p520-533, DOI: 10.1061/(ASCE)WR.1943-5452.0000345, 2013

682 Krajewski, W. F., Vignal, B.: Evaluation of anomalous propagation echo detection in WSR-
683 88D data: A large sample case study, Journal of Atmospheric and Oceanic Technology, Vol.
684 18, 2001

685 Lucas, W. C. and Sample, D. J.: Reducing combined sewer overflows by using outlet controls
686 for Green Stormwater Infrastructure: Case study in Richmond, Virginia, Journal of
687 Hydrology, Vol. 520, p473-488, DOI: 10.1016/j.jhydrol.2014.10.029.

688 Lyandres, O. and Welch, L. C.: Reducing combined sewer overflows in the Great Lakes: Why
689 investing in infrastructure is critical to improving water quality, 2012

690 Mandapaka, P. V. and Qin, X.: Analysis and characterization of probability distribution and
691 small-scale spatial variability of rainfall in Singapore using a dense gauge network, Journal of
692 Applied Meteorology & Climatology, Vol. 52, Issue 12, p2781-2796, DOI: 10.1175/JAMC-
693 D-13-0115.1, 2013

694 Mailhot, A., Talbot, G. and Lavallée, B.: Relationships between rainfall and Combined Sewer
695 Overflow (CSO) occurrences, Journal of Hydrology, Vol. 523, p602-609, DOI:
696 10.1016/j.jhydrol.2015.01.063., 2015

697 Mamo, T. G.: Evaluation of the potential impact of rainfall intensity variation due to climate
698 change on existing drainage infrastructure, Journal of Irrigation and Drainage Engineering,
699 Vol. 141, Issue 10, p1-7, DOI: 10.1061/(ASCE)IR.1943-4774.0000887, 2015

700 Martinez, A. M. and Kak, A. C.: PCA versus LDA, IEEE Transactions on Pattern Analysis
701 and Machine Intelligence, Vol. 23, Issue 2, p228-233, DOI:10.1109/34.908974, 2001

702 Montalto, F., Behr, C., Alfredo, K., Wolf, M., Arye, M., and Walsh, M.: Rapid assessment of
703 the cost-effectiveness of low impact development for CSO control, Landscape and Urban
704 Planning, 82(2007)117-131, dx.doi.org/10.1016/j.landurbplan.2007.02.004, 2007

705 Morin, E., Krajewski, W. F., Goodrich, D. C., Gao, X., and Sorooshian, S.: Estimating
706 Rainfall Intensities from Weather Radar Data: The Scale-Dependency Problem, Journal of
707 hydrometeorology, Vol 4, 2003

708 Morita, M.: Quantification of increased flood risk due to global climate change for urban river
709 management planning, Water Science & Technology, Vol. 63, Issue 12, p2967-2974, DOI:
710 10.2166/wst.2011.172, 2011
711 Mounce, S.R., Shepherd, W., Sailor, G., Shucksmith, J., and Saul, A.J.: Predicting combined
712 sewer overflows chamber depth using artificial neural networks with rainfall radar data, Water
713 Science & Technology, 69(6):1326-1333, 2014
714 MSD: CSO characteristics report-Combined Sewer Overflow Fact Sheet (CSO130),
715 Metropolitan Sewer District (MSD), Louisville, Kentucky, 2014
716 Peter, J. R., Manton, M. J., Potts, R. J., May, P. T., Collis, S. M., and Wilson, L.: Radar-
717 derived statistics of convective storms in Southeast Queensland, Journal of applied
718 meteorology & climatology, Vol. 54, Issue 10, p1985-2008, DOI: 10.1175/JAMC-D-13-
719 0347.1, 2015
720 Price, K., Purucker, S. T., Kraemer, S. R., Babendreier, J. E. and Knighters, C. D.:
721 Comparison of radar and gauge precipitation data in watershed models across varying spatial
722 and temporal scales, Hydrological Processes, Vol. 28, No. 9, p3505-3520, 2014
723 Qi, Y., Martinaitis, S., Zhang, J., Cocks, S.: A real-time automated quality control of hourly
724 rain gauge data based on multiple sensors in MRMS system, Journal of Hydrometeorology,
725 Vol. 17, Issue 6, p1675-1691, DOI: 10.1175/JHM-D-15-0188.1., 2016
726 Romnée, A., Evrard, A. and Trachte, S.: Methodology for a stormwater sensitive urban
727 watershed design, Journal of Hydrology, Vol. 530, p87-102, DOI:
728 10.1016/j.jhydrol.2015.09.054, 2015
729 Sangam, S., Futaba, K., Takashi, N.: Use of principal component analysis, factor analysis and
730 discriminant analysis to evaluate spatial and temporal variations in water quality of the
731 Mekong River, Journal of Hydroinformatics, Vol. 10, Issue 1, p43-56, 2008

732 Seo, D. J., Breidenbach, J., Fulton, R., and Miller, D.: Real-time adjustment of range-
733 dependent biases in WSR-88D rainfall estimates due to nonuniform vertical profile of
734 reflectivity, Journal of Hydrometeorology, Vol 1, 2000

735 Tahmasebi, P., Hezarkhani, A., and Mortazavi, M.: Application of discriminant analysis for
736 alteration separation; sungun copper deposit, East Azerbaijan, Iran, Australian Journal of
737 Basic and Applied Sciences, Vol. 6, Issue 4, p564-576, 2010

738 Ulbrich, C. W. and Lee, L. C.: Rainfall Measurement Error by WSR-88D Radars due to
739 Variations in Z-R Law Parameters and the Radar Constant, Journal of atmospheric and
740 oceanic technology, Vol 16, 1999

741 Vignal, B., Krajewski, W. F.: Large-sample evaluation of two methods to correct range-
742 dependent error for WSR-88D rainfall estimates, Journal of Hydrometeorology, Vol 2, 2001

743 Xie, J., Hone, K., Xie, W., Gao, X., Shi, Y., and Liu, X.: Extending twin support vector
744 machine classifier for multi-category classification problems, Intelligent Data Analysis, Vol
745 17, Issue 4, p649-664, DOI: 10.3233/IDA-130598, 2013

746 Yang, L., Smith, J. A., Wright, D. B., Baeck, M. L., Villarini, G., Tian, F., and Hu, H.:
747 Urbanization and climate change: An examination of nonstationarities in urban flooding,
748 Journal of Hydrometeorology, Vol. 14, Issue 6, p1791-1801, DOI: 10.1175/JHM-D-12-095.1,
749 2013

750 Zawilski, M and Brzeziska, A.: Areal rainfall intensity distribution over an urban area and its
751 effect on a combined sewerage system, Urban Water Journal, Vol. 11, Issue 7, p532-542,
752 DOI:10.1080/1573062X.2013.831909, 2014

753

754

Hydrol. Earth Syst. Sci. Discuss., doi:10.5194/hess-2016-362, 2016
Manuscript under review for journal Hydrol. Earth Syst. Sci.
Published: 30 August 2016

Tables

Table 1. Group Mean Values of Rainfall Characteristics by Discriminant Analysis.

Groups	Variables	Mean
Non-Significant Overflow (group 0)	Duration (hour)	4.57
	Rain Total (mm)	8.85
	Rain Peak (mm/15min)	3.76
	Rain Type (convective ratio)	0.47
	Rain Continuity ratio	0.56
Significant Overflow (group 1)	Duration (hour)	6.14
	Rain Total (mm)	23.7
	Rain Peak (mm/15min)	6.20
	Rain Type (convective ratio)	0.50
	Rain Continuity ratio	0.60
Total Events	Duration (hour)	5.37
	Rain Total (mm)	15.4
	Rain Peak (mm/15min)	4.84
	Rain Type (convective ratio)	0.48
	Rain Continuity	0.58

Hydrol. Earth Syst. Sci. Discuss., doi:10.5194/hess-2016-362, 2016
Manuscript under review for journal Hydrol. Earth Syst. Sci.
Published: 30 August 2016

759 Table 2. Classification Result and Predicted Group Membership by Discriminant Analysis.

Overflow Severity			Predicted Group Membership		Total
			Non-Significant	Significant	
Original	Count	Non-Significant	29	0	29
		Significant	11	12	23
	Percentage	Non-Significant	100	0	100
		Significant	47.8	52.2	100

760

761

762

763

764

765

766

767

768

769

770

771

772

Hydrol. Earth Syst. Sci. Discuss., doi:10.5194/hess-2016-362, 2016
Manuscript under review for journal Hydrol. Earth Syst. Sci.
Published: 30 August 2016

773 **Figures**

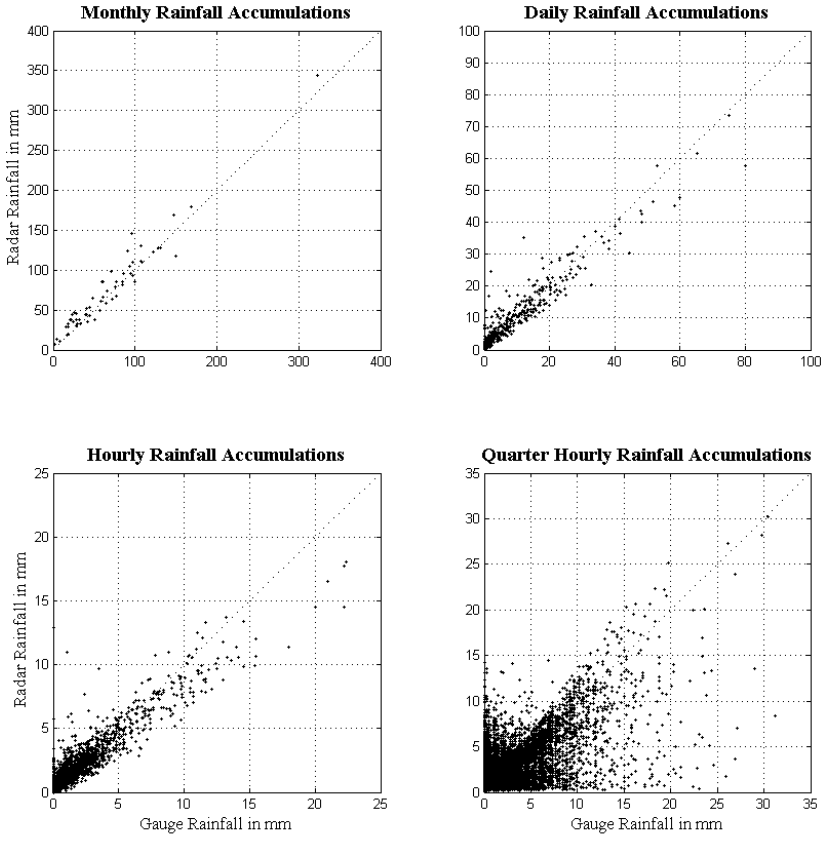

774

775 Figure 1. Gauge and Radar rainfall depth in 2-dimensional space (gauge-radar volume) across
776 temporal resolutions: monthly (upper- left), daily (upper-right), hourly (lower-left), quarter-
777 hourly (lower-right)

Hydrol. Earth Syst. Sci. Discuss., doi:10.5194/hess-2016-362, 2016
Manuscript under review for journal Hydrol. Earth Syst. Sci.
Published: 30 August 2016

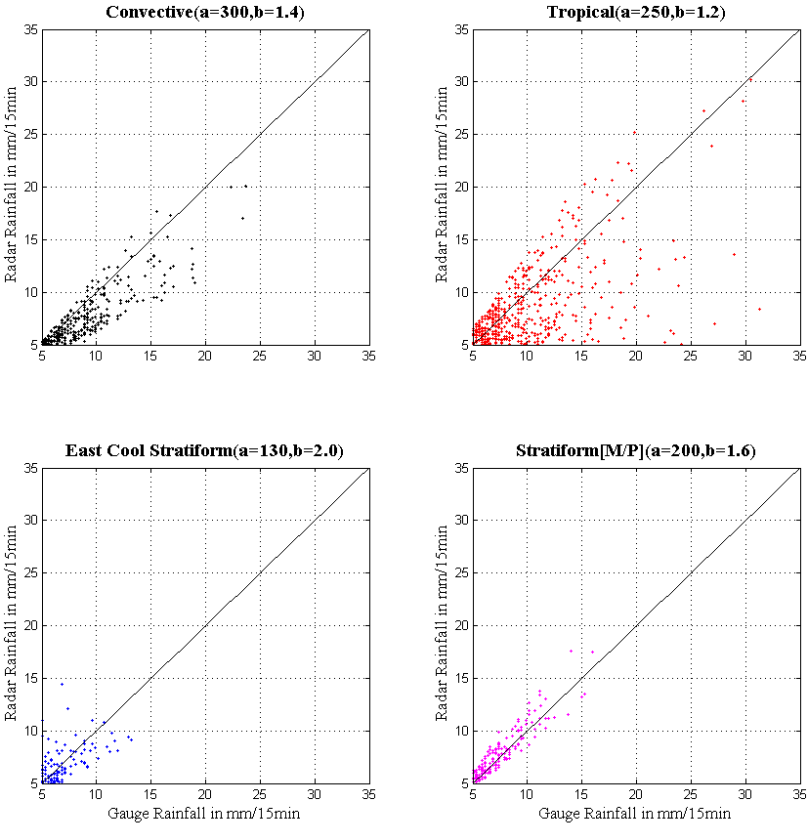

778

779 Figure 2. Scatter plots of rainfall volumes for each storm type after optimization (minimum
780 RMSE error): convective type (upper-left), tropical type (upper-right), east-cool-stratiform
781 type (lower-left), stratiform – Marshall/Palmer - type (lower-right)

Hydrol. Earth Syst. Sci. Discuss., doi:10.5194/hess-2016-362, 2016
Manuscript under review for journal Hydrol. Earth Syst. Sci.
Published: 30 August 2016

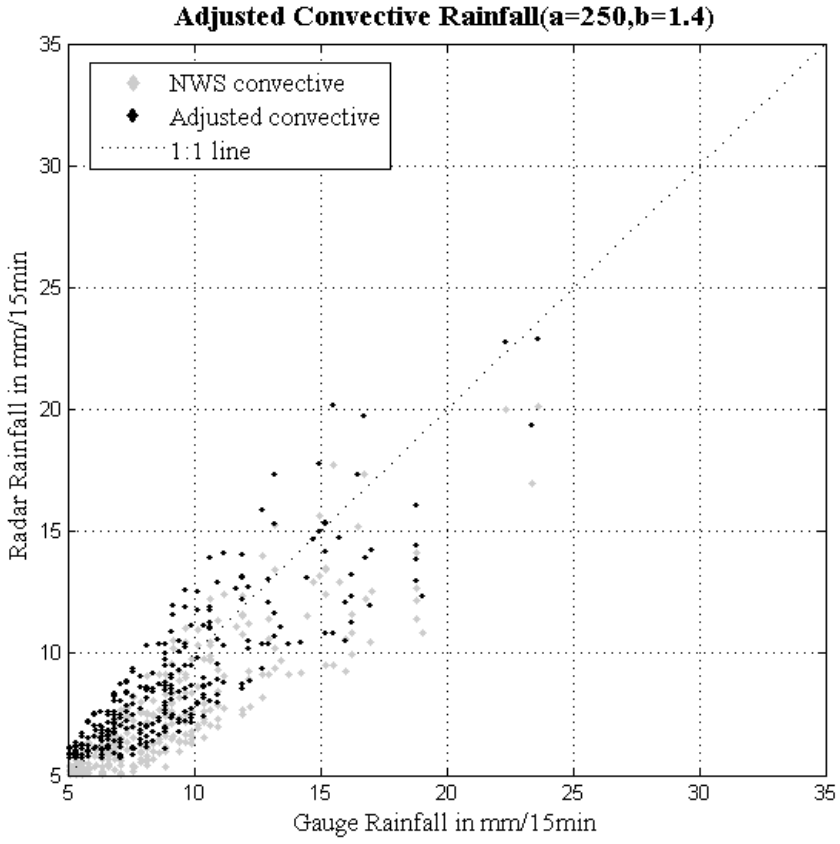

782

783 Figure 3. Convective rainfall type: radar and gauge comparison with (a) standard NWS Z-R

784 relation (light shade marker), and (b) optimized Z-R relation (minimum RMSE error)

Hydrol. Earth Syst. Sci. Discuss., doi:10.5194/hess-2016-362, 2016
Manuscript under review for journal Hydrol. Earth Syst. Sci.
Published: 30 August 2016

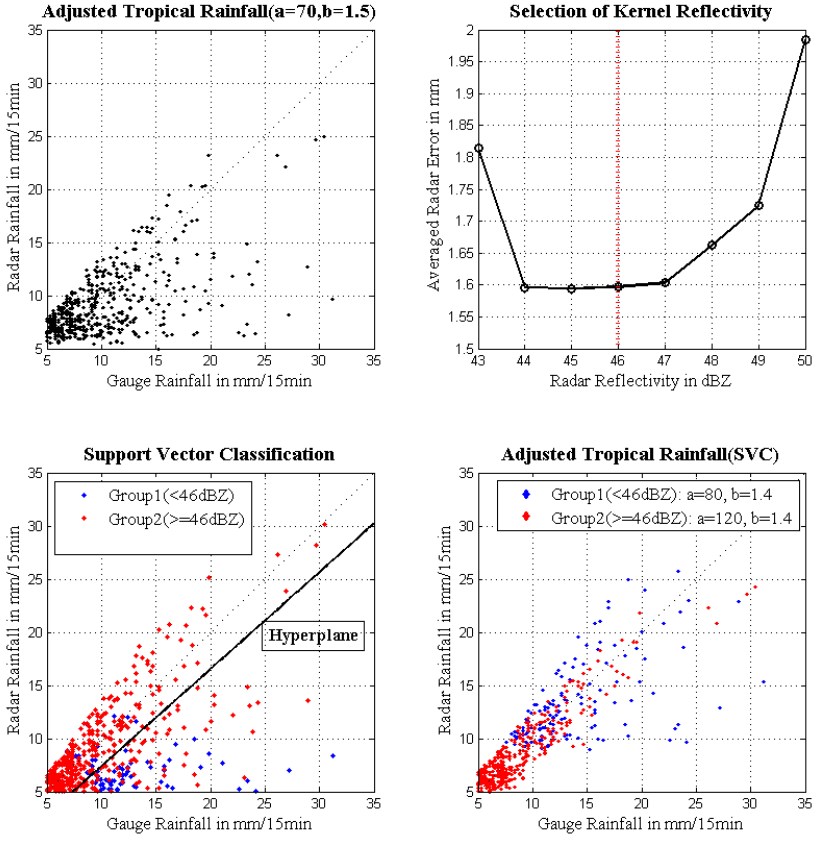

785

786 Figure 4. Tropical type rainfall results: Optimized minimum RMSE error (upper-left);
787 Decision schematic for SVC kernel within least RMSE error range (upper-right); SVC binary
788 clustering hyperplane (lower-left), SVC-based optimization with two rainfall groups (lower-
789 right)

Hydrol. Earth Syst. Sci. Discuss., doi:10.5194/hess-2016-362, 2016
Manuscript under review for journal Hydrol. Earth Syst. Sci.
Published: 30 August 2016

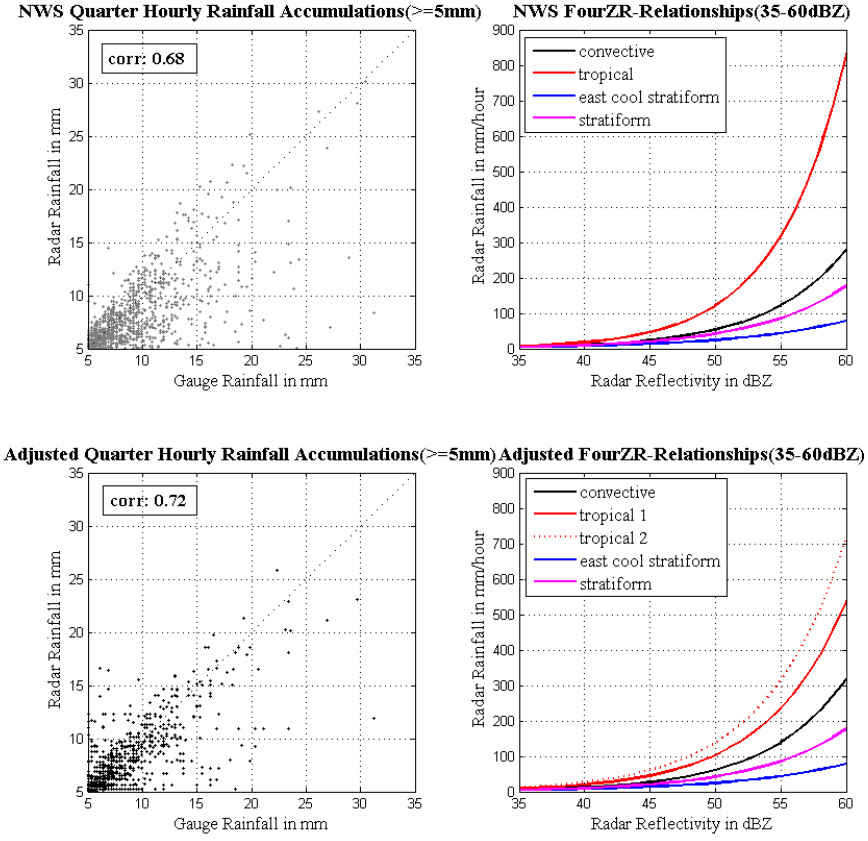

790

791 Figure 5. Comparison of local radar rainfall estimations and corresponding Z-R relationships:
792 (NWS Standardized Z-R-based quarter-hourly rainfall accumulation (upper-left); four
793 empirical NWS Z-R relationships (upper-right); Optimal SVC-based quarter-hourly rainfall
794 accumulation (lower-left); SVC-based optimal Z-R relationships (lower-right) (adapted from
795 Hyun et al., 2016c).

796

Hydrol. Earth Syst. Sci. Discuss., doi:10.5194/hess-2016-362, 2016
Manuscript under review for journal Hydrol. Earth Syst. Sci.
Published: 30 August 2016

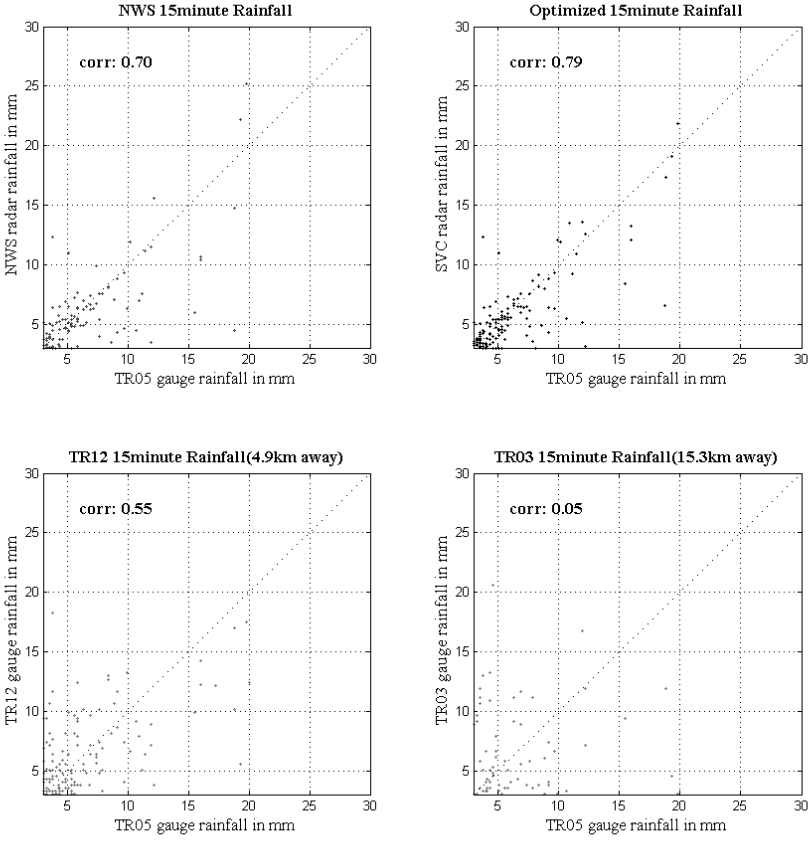

797

798 Figure 6. Rainfall data quality comparisons with the reference rainfall data (TR05): NWS
799 radar data (upper-left), Quality-improved radar data by SVC (upper-right), MSD rain gauge-
800 TR12; 4.9km away from the study area (lower-left), and MSD rain gauge-TR03; 15.3km
801 away from the study area (lower-right).

802

Hydrol. Earth Syst. Sci. Discuss., doi:10.5194/hess-2016-362, 2016
Manuscript under review for journal Hydrol. Earth Syst. Sci.
Published: 30 August 2016

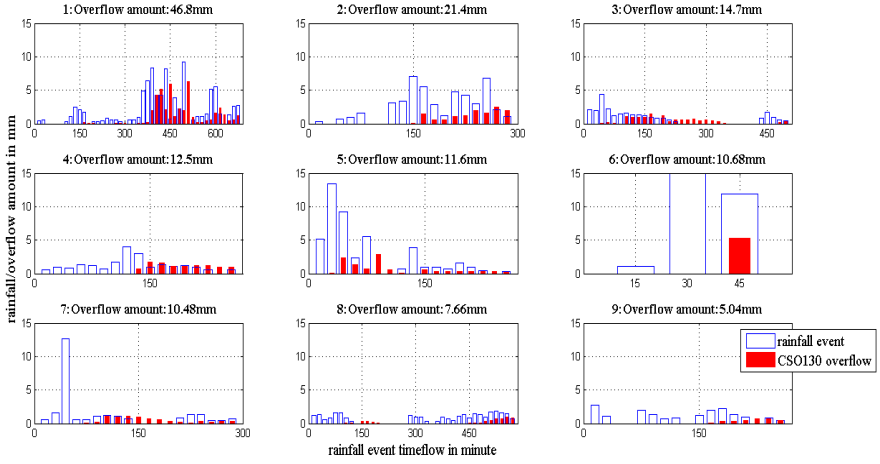

803

804 Figure 7. Selected CSO events and corresponding rainfall events; Event number denotes the
805 rank of the overflow amount through the outfall structure to Beargrass Creek, Louisville, KY.

806

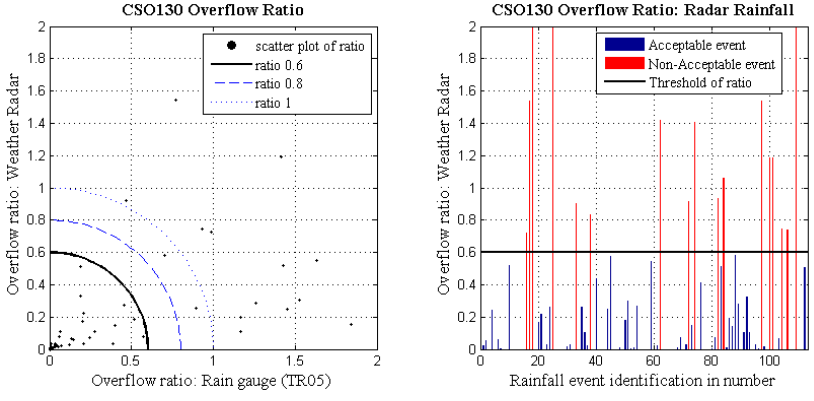

807

808 Figure 8. Overflow ratio plots. Left side: Two-dimensional radar & gauge rainfall field; x-axis
809 shows rain gauge ratio-MSD TR05 (nearest study area), y-axis shows radar ratio-NWS
810 weather radar KLVX. Right side: Criteria threshold for valid event selection: 52 acceptable
811 events (blue) below the 0.60 overflow/rainfall threshold, and 43 non-acceptable events (red)
812 exceed the threshold.

Hydrol. Earth Syst. Sci. Discuss., doi:10.5194/hess-2016-362, 2016
Manuscript under review for journal Hydrol. Earth Syst. Sci.
Published: 30 August 2016

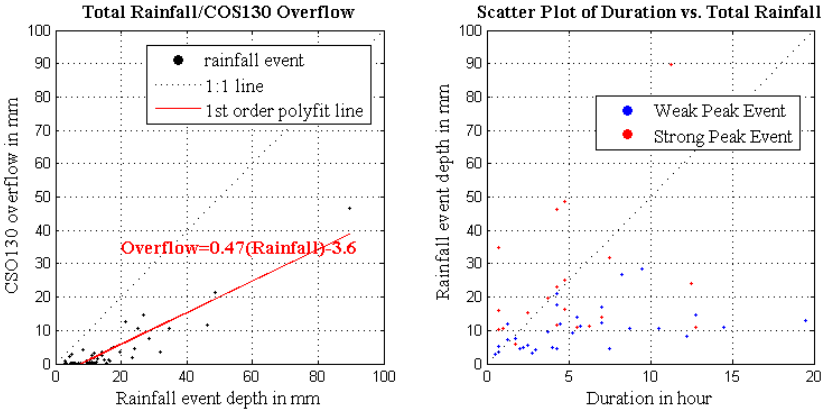

Figure 9. Event-based rain depth versus overflow depth (left), and rain event duration versus rainfall depth grouped by peak rain intensity (right). Intensity threshold peak is 4.87mm/15minute to identify weak (blue) and strong (red) peak event groups.

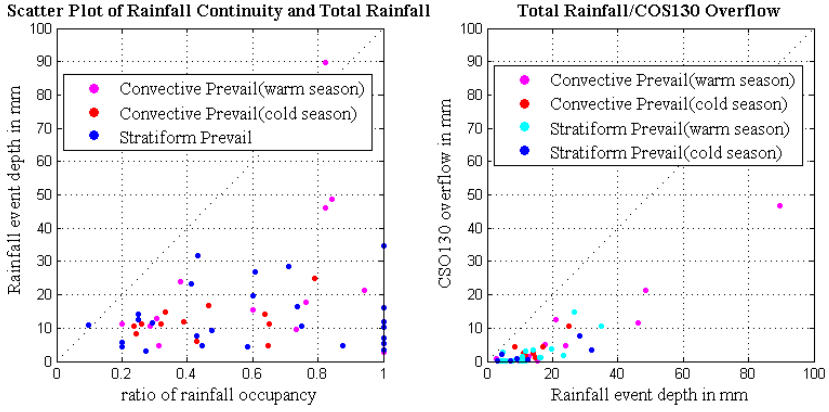

Figure 10. Rainfall occupancy ratio (ratio of continuous rain duration to total event duration) and total rainfall event depth: convective event type in warm season (magenta), convective type in cold season (red) and stratiform (blue) (left). Event-based rainfall depth versus

Hydrol. Earth Syst. Sci. Discuss., doi:10.5194/hess-2016-362, 2016
Manuscript under review for journal Hydrol. Earth Syst. Sci.
Published: 30 August 2016

824 overflow depth: convective-warm season (magenta), convective-cold season (red), stratiform-
825 warm season (cyan), and stratiform-cold season (blue) (right).

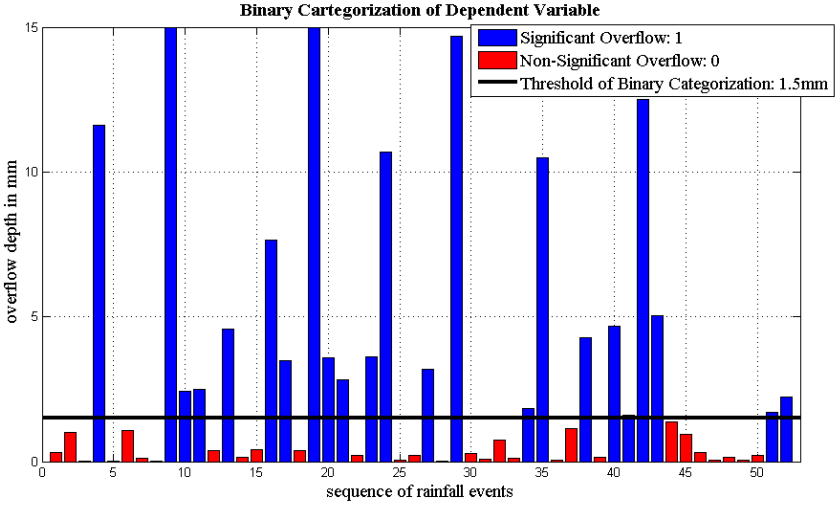

826

827 Figure 11. Overflow event and 1.5-mm depth threshold separating overflow events into two
828 binary categories – significant (denoted as 1) and non-Significant (denoted as 0).